Available online at www.sciencedirect.com
SCIENCE DIRECT®
Chemical Physics Letters 413 (2005) 10–15
CHEMICAL PHYSICS LETTERS
www.elsevier.com/locate/cplett

Light emission spectroscopy of self-assembled arrays of silver nano-crystals with the STM

N. Nilius [a,*], H.-M. Benia [a], C. Salzemann [a], G. Rupprechter [a], H.-J. Freund [a], A. Brioude [b], M.-P. Pileni [b]

[a] *Fritz-Haber-Institut der Max-Planck-Gesellschaft, Department of Chemical Physics, Faradayweg 4-6, D14195 Berlin, Germany*
[b] *Laboratoire des Materiaux Mesoscopiques et Nanometriques, URA CNRS 7070, Universite Pierre et Marie Curie, BP 52,4 Place Jussieu, 75005 Paris, France*

Received 5 April 2005; in final form 22 June 2005
Available online 8 August 2005

Abstract

The optical properties of ordered and disordered assemblies of Ag nano-crystals on HOPG have been characterized by photon emission spectroscopy with the STM. The spectra reveal two emission maxima, which are attributed to plasmon modes oscillating parallel and perpendicular to the substrate plane. The interpretation of the emission mechanism is supported by polarization measurements and model calculations. The effect of long-range order in the particle layer on the optical properties is discussed.

In analogy to the formation of bulk crystals from single atoms, well-ordered two- and three-dimensional (2D, 3D) super-lattices can be aggregated from nano-particles with small size distribution [1–4]. The properties of these supra-crystals dramatically deviate from those of the isolated objects. Static and dynamic electromagnetic dipoles in the individual particles couple in the ensemble and stimulate the formation of new delocalized modes. Such collective excitations dominate the optical [5–7], magnetic [8] and vibronic properties of the supra-crystals [9]. The development of collective modes depends on the nature and efficiency of the coupling mechanism, the lattice constant and the long-range order in the network. Control over these parameters allows certain adjustment of the ensemble properties, opening the way to tailor novel materials with potential applications in optical and storage devices.

Intensive investigations of 2D self-organizations were initiated by the first development of reliable soft-chemical ways for their fabrication [1,4,10]. The synthesis is commonly based on a reverse micelle technique. The small size distribution of the so-prepared nano-crystals stimulates self-assembling when deposited onto a flat surface. Using this approach, well-ordered 2D and 3D particle ensembles were fabricated from various materials (e.g., Ag, Au, Co, $BaFeO_3$, CdS), and characterized by a wide spectrum of surface science techniques [1–11].

Self-organizations of Ag particles have become a model system to study the development of collective optical modes in supra-crystals. The optical response of an isolated Ag cluster is dominated by coherent oscillations of its electron gas (Mie plasmon), giving rise to distinct maxima in extinction spectra [12]. Electromagnetic coupling between neighboring particles results in a splitting and shift of the plasmon resonance, induced by constructive interference of the in-plane dipoles and destructive coupling of the out-of-plane modes. This phenomenon has been observed by extinction spectroscopy on lithographically prepared particle arrays as well as on disordered cluster ensembles [13,14]. For self-assembled Ag nano-crystals on HOPG, UV–VIS

* Corresponding author. Fax: +49 30 8413 4101.
E-mail address: nilius@fhi-berlin.mpg.de (N. Nilius).

0009-2614/$ - see front matter © 2005 Elsevier B.V. All rights reserved.
doi:10.1016/j.cplett.2005.06.127

reflection spectroscopy has been reported [6,7]. The interpretation of reflectance data is not straightforward, as single (e.g., interband transitions) as well as collective excitations (plasmons) contribute to the spectral response. Information on energy and line width of characteristic collective modes was therefore provided by model calculations, solving Maxwell's equations for a hexagonal particle network [15,16].

In this Letter, the optical properties of 2D super-lattices of Ag nano-crystals are investigated by photon emission spectroscopy with a scanning tunneling microscope (STM) [17]. The light emission is excited by field-emitted electrons form the STM tip. The huge oscillator strength associated to plasmon modes makes emission spectroscopy especially sensitive to collective electronic excitations in the particle ensemble. The combination of STM and photon spectroscopy allows direct correlation between topography and optical properties of a localized surface area. As the size of the probed area is controlled via the tip-sample distance, emission spectroscopy with the STM can be performed on extended particle ensembles as well as on single particles on the surface.

The experiments are carried out with a beetle-type STM operated at room temperature and ultra-high vacuum conditions ($p < 5 \times 10^{-10}$ mbar) [18]. The microscope head is surrounded by a parabolic mirror, which collects the photons emitted from the tunneling junction. A second mirror outside the vacuum chamber focuses the light onto the entrance slit of a grating spectrograph attached to a liquid-nitrogen cooled CCD detector. The polarization of the emitted light is measured with a Glenn–Thompson polarization prism. Due to the large acceptance angle of the optical system and the high quantum efficiency of the CCD chip, detection and spectral analysis of extremely small photon intensities is achieved down to some hundred photons per second [18]. Ag nano-crystals are synthesized in reverse micelles [19]. After extraction from the micellar solution, they are coated with dodecanethiol and dispersed in hexane. The particle size is controlled by a size-selective precipitation technique, which reduces the size distribution to approximately 8% with 5 nm mean particle diameter. A few micro-liter of low-concentrated colloidal solution is dropped onto a flat HOPG surface, freshly prepared by stripping off several graphite layers with adhesive tape. The small size distribution of the nano-crystals induces self-organization into a hexagonal network with 7 nm lattice constant (Fig. 1a). No long-range order develops on the HOPG when a poly-

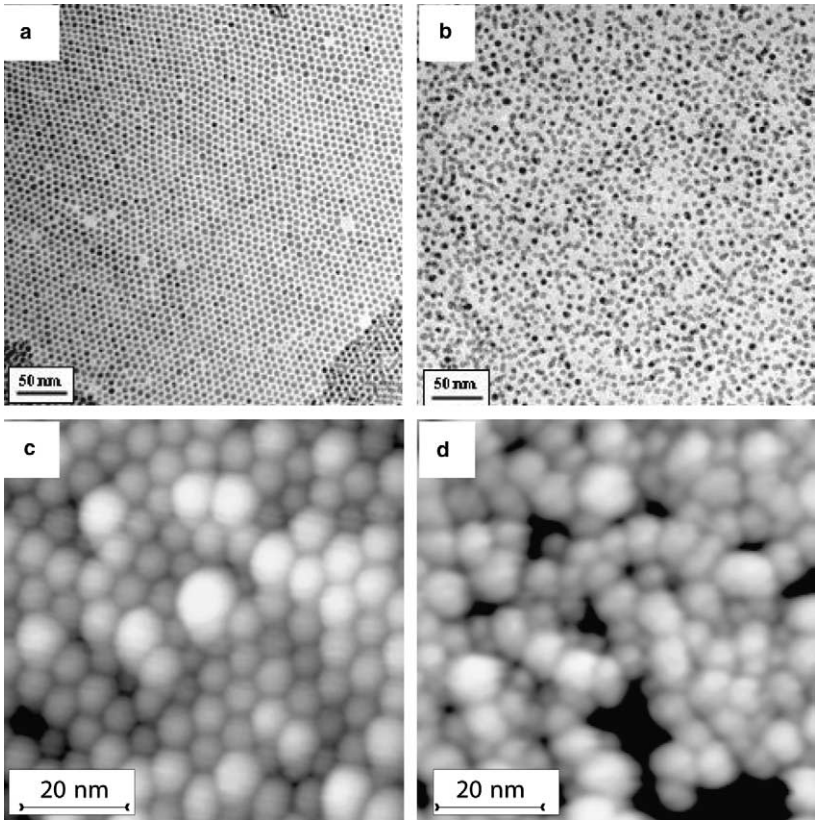

Fig. 1. TEM images of a monolayer of Ag nano-crystals on HOPG with (a) a small and (b) a large particle size distribution. Image sizes are 400×400 nm^2. (c and d) STM topographic images of identically prepared particle ensembles as in (a) and (b). Tip bias and electron current were set to -0.4 V and 0.5 nA, respectively. Image sizes are 75×75 nm^2.

disperse colloidal solution is used (Fig. 1b). The samples are introduced into the vacuum roughly 1 h after deposition.

The topology of Ag nano-crystal assemblies is characterized by STM images taken in the constant-current mode. Imaging is possible only at relatively mild tunneling conditions ($U < 1.5$ V, $I < 1$ nA), manifesting the weak coupling of the Ag particles to the HOPG support. STM images of a single layer of mono- and poly-disperse nano-crystals are shown in Fig. 1c and d, respectively. The important role of the size distribution for long-range order in the ensemble is obvious. Light emission is stimulated by injection of field-emitted electrons from the STM tip. The electron current is adjusted to 1 nA by retracting the tip several 100 nm from the surface and applying a moderate negative bias. The field-emitted electrons spread over a wide surface area ranging between 10.000 and 100.000 nm^2 and coherently excite an ensemble of Ag particles. Due to low current densities and short irradiation times of 60 s per spectrum, no electron-induced damage is observed in STM images taken after each spectroscopic run. Light emission spectra recorded from a 2D super-lattice of Ag nano-crystals are shown in Fig. 2a for different tip voltages. The emission spectra are characterized by a maximum at 345 nm (3.6 eV) and a shoulder around 500 nm (2.5 eV) [20]. The full-width-at-half-maximum (FWHM) of the high-energy peak is approximately three times smaller than the low-energy peak width. The total emission yield increases exponentially with the electron energy, but linearly with the current between tip and sample. Photon emission spectra from a disordered particle ensemble show a qualitatively similar behavior with the main peak slightly blue-shifted to 340 nm (3.65 eV) (Fig. 2b). The most pronounced difference is the reduced intensity of the 2.5 eV shoulder. While the intensity ratio between low- and high-energy feature amounts to

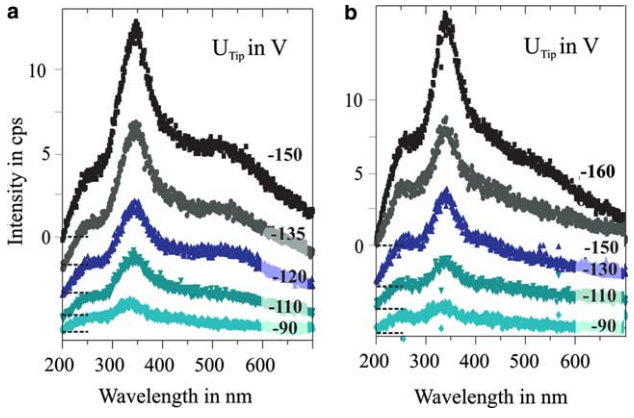

Fig. 2. Photon emission spectra of (a) an ordered and (b) a disordered monolayer of Ag nano-crystals on HOPG excited by field-emitted electrons with different kinetic energy. The electron current was set to 1 nA.

roughly 0.45 for ordered arrays, it drops to 0.38 for disordered ensembles [20]. Only a weak and broad emission line around 500 nm is detected for bare HOPG prior to the particle deposition.

Electron-induced light emission from Ag particles is a well-known phenomenon and has been intensively investigated by experiment and theory [12,17,21]. The emission results from a radiative decay of coherent oscillations in the particle electron gas (Mie plasmons), excited by the injection of electrons. The plasmon energy is determined by size and shape of the particles as well as by the dielectric properties of particle material $\varepsilon_{Ag}(\omega)$ and environment ε_m. It can be approximated from the polarizability of a metal sphere with radius r immersed in a homogeneous dielectric medium [12]

$$\alpha(\omega) \propto r^3 \frac{\varepsilon_{Ag}(\omega) - \varepsilon_m}{\varepsilon_{Ag}(\omega) + 2\varepsilon_m}. \quad (1)$$

For an isolated sphere, the plasmon energy is threefold degenerated due to equivalent polarizabilities along the three major axes. Using the dielectric constant for the dodecanethiol shell ($\varepsilon_m = 2$), a fundamental mode at 3.15 eV is calculated for a single Ag sphere [6,22]. Deposition onto a surface lifts the degeneracy and splits the plasmon into two modes, oriented parallel (1,1) and perpendicular (1,0) to the support. For a spherical, ligand-stabilized Ag particle on HOPG, substrate-induced effects are small and account only for some 10 meV splitting of the fundamental excitation [16]. The organization of Ag nano-crystals into a 2D network strongly increases the separation between both plasmon modes due to dipolar interactions in the layer. In-plane dipoles experience constructive interference, which increases the polarizability along this direction and shifts the (1,1) plasmon to lower energies. Out-of-plane dipoles interfere destructively, leading to a reduced polarizability perpendicular to the support and a blue-shifted (1,0) Mie mode. The energy separation between both modes sensitively depends on the strength of the dipolar interaction and therefore on the inter-particle distance. The effect can be approximated with an effective medium theory, as formulated by Barrera and Russier [15,16] for square and hexagonal particle arrays. Here, the plasmon modes show up as maxima in the imaginary part of the effective ensemble polarizability for the (1,1) and (1,0) directions [6]:

$$\varepsilon_{eff}^{(1,1)} \propto \frac{1 - (\lambda S_0 \alpha(\omega)/16) + (\pi/\sqrt{3})(2r/d)^2 \alpha(\omega)}{1 - (\lambda S_0 \alpha(\omega)/16)}, \quad (2a)$$

$$\varepsilon_{eff}^{(1,0)} \propto \frac{1 + (\lambda S_0 \alpha(\omega)/8)}{1 + (\lambda S_0 \alpha(\omega)/8) - (\pi/\sqrt{3})(2r/d)^2 \alpha(\omega)}$$

$$\text{with } \lambda = \left(\frac{2r}{d}\right)^3. \quad (2b)$$

The formula includes the lattice sum of a hexagonal lattice $S_0 = 11.034$, the particle radius $r = 2.5$ nm and the

lattice constant $d = 7$ nm. The single-particle polarizability $\alpha(\omega)$ is calculated from experimentally determined dielectric functions using Eq. (1) [22]. For a well-ordered hexagonal ensemble of Ag nano-crystals, the energies of the out-of-plane and in-plane plasmon modes are determined to 3.4 and 2.7 eV, respectively.

Based on this estimate, we can safely assign the high-energy peak in the experiments to the (1,0) Mie plasmon with perpendicularly oriented dipoles, whereas the low-energy peak refers to the (1,1) plasmon. The measured mode splitting of 1.1 eV is slightly larger than the calculated value of 0.7 eV. The difference is mainly attributed to an inadequate description of the single-particle polarizability $\alpha(\omega)$, which treats the environment as homogeneous medium and neglects the actual stacking of the dielectric layers. Additional deviations may arise from the use of simplified dielectric functions for the ligand shell and the HOPG. Reflection spectroscopy on identically prepared samples revealed a similar splitting of 1.0 eV between parallel and perpendicular plasmon modes [4,7].

No unambiguous correlation between plasmon energy and long-range order in the particle ensemble could be established from the experimental spectra. The splitting of the Mie plasmon is a subtle indicator for changes in the particle density, but seems to be less sensitive to the particle arrangement in the layer. The average inter-particle distance was found to be comparable in ordered and disordered ensembles, which might explain the similar plasmon energies observed for both preparations. On the other hand, small variations in the plasmon position are likely to be covered by the large FWHM of the experimental peaks. The absence of long-range order in a poly-disperse ensemble is, however, reflected in the observed intensity loss of the 2.5 eV shoulder [23]. In a perfect hexagonal network, the (1,1) mode gains intensity with respect to the (1,0) mode, because of the constructive enhancement of in-plane oscillations and the destructive interference of out-of-plane modes. In assemblies with broader size distribution, this effect is partly suppressed due to a certain detuning of the plasmon energies and a reduced coupling efficiency between neighboring dipoles. Consequently, the intensity ratio between (1,1) and (1,0) emission peaks decreases in ensembles without long-range order, in agreement with the experimental observations (Fig. 2) [23].

The assignment of the high-energy peak to the (1,0) Mie mode is verified by polarization measurements on Ag nano-crystal assemblies. Fig. 3a displays the polarization dependence in emission spectra of a well-ordered particle layer, obtained after subtraction of a polarization independent background. The emission peak shows the expected intensity variation with polarization angle ϕ for linear polarized light [24]: $I(\phi) = I_0 \sin^2\phi$ (Fig. 3b). The polarization vector corresponds to the

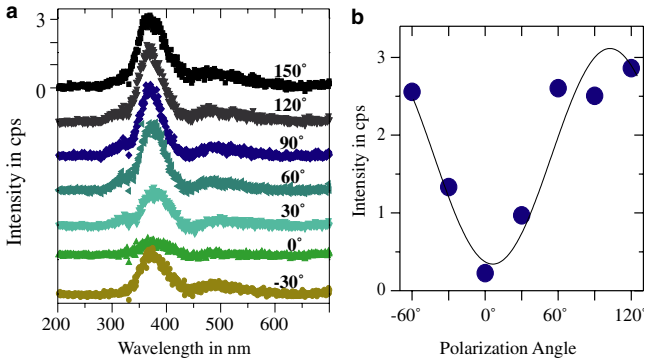

Fig. 3. (a) Polarization dependence of the light emission from an ordered monolayer of Ag nano-crystals on HOPG excited by field-emitted electrons from the STM tip. Tip bias and electron current were set to −220 V and 1 nA, respectively. Polarization angles are given in the figure. Due to the presence of the polarization prism, peak positions are slightly shifted. (b) Intensity of the main peak in (a) as a function of polarization angle. The intensity variation follows the expected behavior for linear polarized light (solid curve).

one of p-polarized light, which is compatible to an emission process from the perpendicularly oscillating dipoles of the (1,0) Mie plasmon. The small emission yield of the low-energy peak and background intensity in this energy range prevented similar investigations for the (1,1) Mie mode.

The interpretation of emission spectra from Ag nano-crystal layers is further supported by experiments on diluted cluster ensembles, where dipole–dipole interactions are supposed to be small. Samples with low particle density are prepared by in situ deposition of Ag atoms onto ultra-thin Al_2O_3 films grown on NiAl(1 1 0) [17,25]. On the inert oxide surface, only step edges act as nucleation centers for the incoming Ag atoms. The resulting cluster density of 3×10^{11} cm^{-2} is 10 times smaller than in the self-assembled particle network on HOPG. Characteristic photon emission spectra from both, a diluted particle ensemble on Al_2O_3 and a dense array of nano-crystals on HOPG are shown in Fig. 4a,c. In contrast to the two emission peaks observed for the 2D self-organizations (3.6 and 2.5 eV), only a single line at 355 nm (3.5 eV) is detected for oxide-supported cluster ensembles. The 3.5 eV-peak emits p-polarized light and is also assigned to photon emission mediated by (1,0) Mie plasmons. The role of dipolar coupling in both ensembles is not easily extracted from the peak positions, because of the additional influences of particle geometry and environment. However, spherical particle shapes and a polarizable ligand-shell would favor lower (1,0) plasmon energies for the self-assembled nano-crystals than for the oxide-supported cluster ensemble. The instead-observed higher mode energy for the 2D super-lattice emphasizes the importance of dipole–dipole interactions in the dense hexagonal network. More obvious is the absence of the (1,1) mode

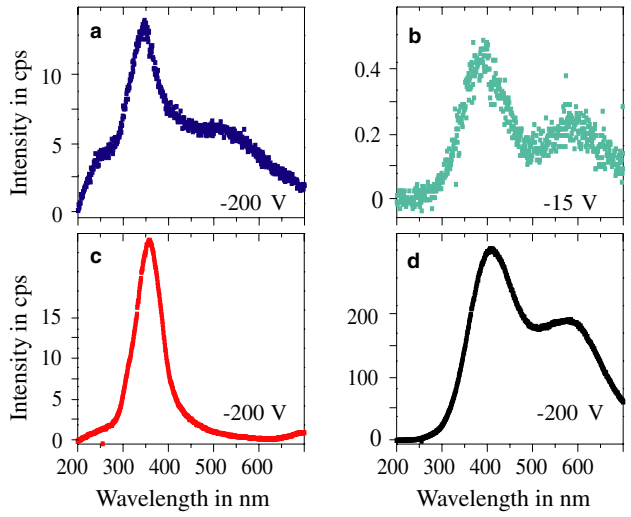

Fig. 4. Photon emission spectra of an ordered layer of Ag nano-crystals on HOPG excited by field-emitted electrons at a tip bias of (a) −200 V ($I = 1$ nA) and (b) −15 V ($I = 5$ nA). Whereas the photon emission in (a) originates from a particle ensemble, only a single particle is excited in (b). Photon emission spectra of (c) bare Ag clusters on Al_2O_3/NiAl(1 1 0) and (d) a multilayer of Ag nano-crystals on HOPG, obtained under identical excitation conditions ($U_{tip} = -200$ V, $I = 1$ nA). Notice the large differences in the emitted intensities in (a–d).

in spectra obtained from Ag clusters on Al_2O_3/NiAl. Cluster densities on the oxide are too small to induce sufficient mode enhancement by constructive interference of the parallel oriented dipoles. The (1, 1) mode falls below the detection limit for the diluted cluster ensemble on the Al_2O_3 film, but remains detectable for the dense Ag nano-crystal network.

Photon emission spectroscopy with the STM allows optical characterization of small particle ensembles down to a single particle on the surface. For a bias voltage of 15 V, the tip-sample gap decreases to approximately 2 nm and only a single cluster is excited by electron injection from the tip [17]. To keep measurable photon yields at low-bias conditions, an electron current of 5 nA has to be used for spectroscopy, although high current densities easily initiate structural damage in the particle layer. A photon-emission spectrum of a single Ag particle in a 2D self-organization is shown in Fig. 4b. The emission characteristic is similar to spectra obtained with higher electron energy, and reveals also two peaks at 390 nm (3.15 eV) and 590 nm (2.1 eV). Whereas the high-energy peak is attributed to the (1, 0) Mie plasmon, the origin of the low-energy peak is rather vague. Photon emission mediated by (1, 1) Mie plasmons was not reported for a single particle before, because of the low excitation cross-section for this mode in the STM [17,23]. The 2.1 eV peak observed here is more likely the result of a coupled electromagnetic mode between tip and sample (tip-induced plasmon) and does not represent an intrinsic excitation of the Ag particle. The position of the (1, 0) plasmon is systematically red-shifted by 0.45 eV with respect to spectra obtained at far-field excitation conditions. This modified position does, however, not correspond to the plasmon energy of an isolated particle, because dipole oscillations in the excited object also couple to image dipoles in the 2D network, thus shifting the mode towards the ensemble value. In fact, the lowering of the plasmon energy is attributed to the small tip-sample distance at −15 V tip bias, which sandwiches the Ag particle between two macroscopic electrodes and dramatically increases the polarizability of its environment. The observed red-shift is therefore interpreted as a result of the enhanced electromagnetic interactions between Ag particle and metallic tip [26,27].

Finally, the optical properties of a multilayer of Ag nano-crystals shall be addressed. Thicker films are prepared by dropping high-concentrated colloidal solution onto the HOPG support. Based on the concentration required for monolayer deposition, the resulting film thickness is estimated to 5–10 layers. The insufficient conductance of thicker films prevents the recording of STM topographic images. Optical spectroscopy is, however, possible due to the increased mean free path of field-emitted electrons with high kinetic energy. Fig. 4d displays an emission spectrum of a multilayer of mono-disperse Ag nano-crystals on HOPG. The total emission yield is 25 times larger compared to monolayer coverage, manifesting the increased number of emission centers on the surface. The double-peak signature of the monolayer is maintained in multilayer spectra; however, peak positions are considerably red-shifted. The high-energy peak is now detected at 405 nm (3.05 eV), the low-energy peak appears at 560 nm (2.2 eV). Simple effective medium theories, such as the Maxwell–Garnett approximation, allow a crude estimation of the polarizability $\varepsilon_{eff}(\omega)$ of a 3D agglomeration from the single-particle polarizability $\alpha(\omega)$ [12]:

$$\varepsilon_{eff}(\omega) \propto \frac{\varepsilon_m - 2f\alpha(\omega)}{\varepsilon_m + 2f\alpha(\omega)}. \quad (3)$$

The formula is valid for small filling factors f, defined as the volume fraction of particles in the film: $f = (V_{particles}/V_{film})$. For the given parameters ($f = 0.27$, $\varepsilon_m = 2$), the plasmon energy for an infinite particle ensemble is calculated to be 0.3 eV lower than for an isolated Ag sphere. The experimental shift is most pronounced for the out-of-plane (1, 0) mode, which is red-shifted by 0.55 eV from its monolayer position. The in-plane oscillations are less affected by the increased film thickness (0.3 eV), because the effective polarizabilty parallel to the surface has nearly saturated in the monolayer. For a large number of particle layers, the energy of in-plane and out-of-plane plasmon modes should converge. The separation between both emission peaks indeed decreases from 1.1 eV for the monolayer to 0.85 eV for

the multilayer. Degenerated energies for the (1,0) and (1,1) plasmon modes are, however, expected for a film thickness, which is much larger than the 5–10 layers investigated in this experiment.

In conclusion, the light emission excited by field-emitted electrons from an STM tip has been recorded from self-assembled layers of Ag nano-crystals on a HOPG surface. The spectra reveal two emission peaks attributed to the excitation of in-plane and out-of-plane plasmon modes. The relative intensities of the observed emission peaks depend on the structural order in the particle layer. The effect of dipolar coupling in the 2D network on the plasmon energies could not directly be measured because of the fixed inter-particle distance. However, model calculations reveal a pronounced plasmon splitting originating from constructive and destructive interference of the single particle modes in the self-assembled array.

References

[1] L. Motte, F. Billoudet, M.P. Pileni, J. Phys. Chem. 99 (1995) 16425.
[2] C.B. Murray, C.R. Kagan, M.G. Bawendi, Science 270 (1995) 5240.
[3] M.J. Hostetler, J.J. Stokes, R.W. Murray, Langmuir 12 (1996) 3604.
[4] M.P. Pileni, J. Phys. Chem. B 105 (2001) 3358.
[5] A.O. Gusev, A. Taleb, F. Silly, F. Charra, M.P. Pileni, Adv. Mater. 12 (2000) 1583.
[6] N. Pinna, M. Maillard, A. Courty, V. Russier, M.P. Pileni, Phys. Rev. B 66 (2002) 045415.
[7] A. Taleb, V. Russier, A. Courty, M.P. Pileni, Phys. Rev. B 59 (1999) 13350.
[8] V. Russier, C. Petit, J. Legrand, M.P. Pileni, Phys. Rev. B 62 (2000) 3910.
[9] A. Courty, A. Mermet, P.A. Albouy, E. Duval, M.P. Pileni, Nat. Mater. 4 (2005) 395.
[10] M.P. Pileni, Y. Lalatonne, D. Ingert, I. Lisiecki, A. Courty, Faraday Discuss. 125 (2004) 251.
[11] S. Maenosono, C.D. Dushkin, S. Saita, Y. Yamaguchi, Langmuir 15 (1999) 957.
[12] U. Kreibig, W. Vollmer (Eds.), Optical Properties of Metal Clusters, Springer Series Materials Science, vol. 25, Springer, Berlin, 1995.
[13] F. Stietz, F. Träger, Philos. Mag. B 79 (1999) 1281; W. Gotschy, K. Vonmetz, A. Leitner, F.R. Aussenegg, Appl. Phys. B 63 (1996) 381.
[14] C.L. Haynes, A.D. McFarland, L. Zhao, R.P. van Duyne, G. Schatz, L. Gunnarsson, J. Prikulis, B. Kasemo, M. Käll, J. Chem. Phys. B 107 (2003) 7337.
[15] R.G. Barrera, M. Delcastillomussot, G. Monsivais, P. Villasenor, W.L. Mochan, Phys. Rev. B 43 (1991) 13819.
[16] V. Russier, M.P. Pileni, Surf. Sci. 425 (1999) 313.
[17] N. Nilius, N. Ernst, H.-J. Freund, Phys. Rev. Lett. 84 (2000) 3994.
[18] N. Nilius, A. Cörper, G. Bozdech, N. Ernst, H.-J. Freund, Prog. Surf. Sci. 67 (2001) 99.
[19] C. Petit, P. Lixon, M.P. Pileni, J. Phys. Chem. B 97 (1993) 12974.
[20] Peak positions and intensities are determined by fitting two GAUSSIANS to the measured spectra. The spectral shoulder at 250 nm is related to transition radiation and Bremsstrahlung resulting from the sudden velocity change of the injected electrons in the sample.
[21] M.S. Chung, T.A. Callcott, E. Kretschmann, E.T. Arakawa, Surf. Sci. 91 (1980) 245.
[22] E.D. Palik (Ed.), Handbook of Optical Constants of Solids, Academic press, Orlando, 1985.
[23] The dominance of the (1,0) peak is the consequence of the specific excitation mechanism in the STM. Field-emitted electrons from the tip follow the surface normal and efficiently induce dipoles with (1,0) orientation. In-plane oscillations are primarily excited by secondary processes, e.g., hot electron decays, leading to an extremely small excitation cross-section. The importance of secondary processes for the STM-induced light emission is manifested by the exponential dependence of the emission yield on the energy of injected electrons. In contrast, the calculated polarizability of well-ordered particle networks is dominated by the (1,1) Mie mode.
[24] L. Bergmann, C. Schäfer (Eds.), Lehrbuch der Experimentalphysik: Optik, vol. 3, de Gruyter, Berlin, 1966.
[25] M. Bäumer, H.-J. Freund, Prog. Surf. Sci. 61 (1999) 127.
[26] R. Berndt, in: R. Wiesendanger (Ed.), Scanning Probe Microscopy, Springer Series Nano-science and Technology, Springer, Berlin, 1998, p. 97.
[27] N. Nilius, N. Ernst, H.-J. Freund, Phys. Rev. B 65 (2002) 115421.